Current Research in Microbial Sciences 8 (2025) 100375

Contents lists available at ScienceDirect

Current Research in Microbial Sciences

journal homepage: www.sciencedirect.com/journal/current-research-in-microbial-sciences

Pathogenic effects of *Streptococcus oralis* intestinal colonization on bladder health in mice

Natsuno Nakamura [a,b,#], Kota Iioka [b,c,#], Hirobumi Morisaki [b], Nobuo Okahashi [b], Mie Kurosawa [b], Haruka Fukamachi [b], Shohei Matsui [d], Takahiro Funatsu [a,e], Hirotaka Kuwata [b], Momoe Itsumi [b,*]

[a] Department of Special Needs Dentistry, Division of Dentistry for Persons with Disabilities, School of Dentistry, Showa University, 2-1-1 Kitasenzoku, Ohta-ku, Tokyo 145-8515, Japan
[b] Department of Oral Microbiology and Immunology, School of Dentistry, Showa University, 1-5-8 Hatanodai, Shinagawa-ku, Tokyo 142-8555, Japan
[c] Department of Perioperative Medicine, Division of Anesthesiology, School of Dentistry, Showa University, 2-1-1 Kitasenzoku, Ohta-ku, Tokyo 145-8515, Japan
[d] Department of Special Needs Dentistry, Division of Medical and Dental Cooperative Dentistry, Showa University, 2-1-1 Kitasenzoku, Ohta-ku, Tokyo 145-8515, Japan
[e] Department of Pediatric Dentistry, School of Dentistry, Showa University, 2-1-1 Kitasenzoku, Ohta-ku, Tokyo 145-8515, Japan

ARTICLE INFO

Keywords:
Streptococcus oralis
Germ-free mice
Bladder
Cystitis
Oxidative stress
Ectopic colonization

ABSTRACT

Streptococcus oralis, a commensal oral *Streptococcus*, is known as an early colonizer of the tooth surface and causes opportunistic infections, such as bacterial endocarditis. However, its pathogenicity remains unclear. This study aimed to investigate the pathogenicity of *S. oralis in vivo* using a mouse model. To establish *S. oralis*-colonized mice, germ-free mice were orally infected with *S. oralis*. After colonization was confirmed, these infected mice were bred, and their offspring were used as *S. oralis*-colonized mice. *S. oralis* was detected only in the intestine of these mice, which exhibited soft stools but no significant inflammation in the examined tissues. Interestingly, *S. oralis*-colonized mice showed higher urination frequency. Bladder tissue analysis in *S. oralis*-colonized mice revealed atrophy, edema, fibrosis, and epithelial denudation. RNA sequencing analysis of the bladder in *S. oralis*-colonized mice indicated higher expression of genes related to chronic inflammation and extracellular matrix organization, and lower expression of genes related to anti-oxidative stress. In this study, we revealed that the commensal bacterium *S. oralis* induces chronic inflammation and fibrosis in the bladder of mice by intestinal colonization. Hence, our findings indicate that *S. oralis* has the potential to affect distal tissue beyond the oral cavity, potentially possessing a pathogenic factor involved in non-bacterial cystitis. This study highlights the potential impact of *S. oralis* on the urinary system of mice.

1. Introduction

Streptococcus oralis is a bacterium commonly found in the oral cavity and is an initial colonizer of the pellicle, a thin film formed on the surface of teeth (Baty et al., 2022). The pellicle is formed by the adsorption of proteins from saliva onto the tooth surface, providing a scaffold for bacterial attachment (Enax et al., 2023). *S. oralis* contributes to the formation of dental plaque by initially adhering to this pellicle, and thereby facilitates colonization by other bacteria (Baty et al., 2022). However, *S. oralis* produces hydrogen peroxide, which inhibits the growth of resident microbiota within the biofilm (Kim et al., 2022). Hydrogen peroxide exerts its antibacterial effect by damaging the bacterial cell membrane. *S. oralis* therefore plays an important role in regulating and maintaining the balance of the microbial environment in the oral cavity. Nonetheless, *S. oralis* can cause systemic disease under certain conditions. It can enter the bloodstream following dental treatment or oral surgical procedures, adhere to the endocardium, and cause endocarditis (Douglas et al., 1993). Previous reports have shown that co-infection with *S. oralis* and *Candida albicans* exacerbates the pathogenicity of *C. albicans* (Xu et al., 2016). This model utilizes

Abbreviations: : GF, germ-free; CVN, conventional; IC, interstitial cystitis; HE, Hematoxylin and Eosin; LPL, Lamina propria lymphocytes; Th1 cells, CD4+IFN-γ+ cells; Th17 cells, CD4+IL-17+ cells; GO, Gene Ontology; BP, biological processes; CC, cellular components; MF, molecular functions; ROS, reactive oxygen species.

* Corresponding author.
E-mail address: momotabe@gmail.com (M. Itsumi).

# Authors equally contributed to this work.

https://doi.org/10.1016/j.crmicr.2025.100375

Available online 14 March 2025

immunosuppression with cortisone acetate. As a result, a bacterial burden was caused by *S. oralis* and *C. albicans*, suggesting that *S. oralis* plays the role of an infectious bacterium. Nevertheless, the pathogenicity of *S. oralis* when it exists as a commensal, not an infectious, bacterium remains unclear.

Germ free (GF) mouse models are used to investigate the physiological effects of specific bacteria in detail without interference from other microorganisms or environmental factors, because these mice have no colonizing microorganisms internally or externally. Various studies have been conducted using GF mice to date. A mixed infection of *Pseudomonas aeruginosa* and *Candida albicans* in GF mice demonstrated that *C. albicans* suppresses the expression of pyochelin and pyoverdine, which are important molecules for binding and transporting iron, processes that are crucial for the survival of *P. aeruginosa* (Lopez-Medina et al., 2015). Experiments with GF mice infected with *Porphyromonas gingivalis* revealed that this microorganism on its own is not responsible for periodontal inflammation, but rather causes inflammatory disease by disrupting the host microbiota (Hajishengallis et al., 2011). Infection with the oral commensal bacterium *S. anginosus* in GF mice has been shown to induce precancerous lesions in the stomach, highlighting the pathogenicity of this particular microorganism (Fu et al., 2024).

Many studies have been conducted on the impact of oral commensal bacteria on systemic health (Graves et al., 2019). Recent microbiome studies indicate that oral bacteria may contribute to diseases of the urinary tract system. It has been reported that *S. anginosus*, which is not typically found in the urine of healthy individuals, was detected in the urine of patients with urgency urinary incontinence (Pearce et al., 2014). This finding suggests that oral bacteria may influence urinary tract health and are a potential cause of urinary incontinence in women. Cystitis, a progressed form of urinary tract infection, is characterized by symptoms such as frequent urination, pain during urination and residual urine. Most cases of cystitis are caused by bacterial infections, such as *Enterococcus faecalis, Escherichia coli* and *Klebsiella pneumoniae* (Qiao et al., 2013). A type of non-bacterial cystitis known as interstitial cystitis (IC) has also been reported to be characterized by chronic bladder pain and pressure, but its etiology is not fully understood. Despite the detection of bacteria such as *Streptococcus* in the urine of some IC patients, bacteria are not considered to be the direct cause of IC (Jacobs et al., 2021). In clinical practice, *S. mitis/oralis* isolated from urine samples has been generally considered a contaminant, but it has been shown that, in patients with compromised immune systems, S. mitis/oralis was a pathogen of UTI, not a contaminant (Zhang et al., 2023). These studies indicate that it is conceivable that a commensal oral Streptococcus, including *S. oralis*, may also affect urinary tract infections and IC.

2. Materials and methods

2.1. Establishment of S. oralis-colonized mice

S. oralis JCM 12997 (ATCC 35037) was obtained from the Japan Collection of Microorganisms at RIKEN BioResource Center (Tsukuba, Japan) (Bridge and Sneath, 1983). GF and conventional (CVN) BALB/c mice were purchased from CLEA Japan, Inc. (Tokyo, Japan) and Sankyo Labo Service Corporation, Inc. (Tokyo, Japan). GF mice were maintained in a bacteria-free environment within vinyl isolators. CVN mice were maintained in specific pathogen-free conditions. Male and female GF mice were orally administered a 100 mM sodium bicarbonate solution, followed by oral administration of an *S. oralis* suspension (2.5×10^7 cfu/mouse) 15 min later. After 1 week, feces from the mice were collected and plated on brain-heart infusion (BHI; Difco, Becton Dickinson, Sparks, MD, USA) agar (Fuji Film Wako, Osaka, Japan). Gram staining was performed to confirm the colonization of *S. oralis*. Mice confirmed to be colonized were bred to produce *S. oralis*-colonized offspring. To confirm that no contamination occurred in the GF mice and *S. oralis*-colonized mice, we performed checks every 4–5 weeks. Fresh fecal samples were collected from the mice and plated on AccuRate™ Sheep Blood Agar (Shimadzu Diagnostics Corporation, Tokyo, Japan) and potato dextrose agar (Eiken Chemical Co. Ltd., Tochigi, Japan), followed by incubation under both aerobic and anaerobic conditions. Additionally, Gram staining was performed on the *S. oralis*-colonized mice to verify the absence of contamination. *S. oralis*-colonized mice were maintained in vinyl isolators until the time of use. Then, 8–25-week-old *S. oralis*-colonized mice and CVN mice were used for subsequent experiments. Mice aged 8–10 weeks were used for RNA analysis, and mice aged 22–25 weeks were used for all other experiments. In all experiments, we used female mice. This study was approved by the Animal Experiment Committee of Showa University (224044). Experiments were conducted in accordance with the guidelines for animal experiments.

2.2. Analysis of Bristol stool form and fecal water content

The characteristics of stools were scored according to the Bristol scale (Lewis and Heaton, 1997). The water content in mouse feces was calculated on the basis of the protocol by Ebisutani et al. (Ebisutani et al., 2020). First, the weight of fresh feces was measured. Then, the feces were dried by heating at 98 °C for 60 min in a tube, and the total weight was measured to calculate the weight of the dried feces. Finally, the percentage of water content was calculated using the formula: (weight of fresh feces − weight of dried feces) / weight of fresh feces × 100).

2.3. Urinary function analysis

Urination frequency and total urine volume were recorded using the Voided Stain on Paper method (Taga et al., 2023). First, urine collected from CVN mice was dropped onto filter paper at a fixed volume, and the area of spread of the urine was analyzed using ImageJ software to create a calibration curve based on volume (Supplementary Figure 1). Next, filter paper was placed on the floor of the cage, and the mice were kept in the cage for 3 h. To avoid urinary variations due to time of day, the experiment was conducted between 2PM and 5PM. After collection, the filter paper was scanned to calculate the number of urinations and the stained area.

2.4. Hematoxylin and eosin (HE) staining

The tissues were fixed in 4 % paraformaldehyde (Fuji Film Wako) and then used to prepare 4 μm frozen sections. The tissue sections were immersed in hematoxylin 3 G (Sakura Finetek, Tokyo, Japan) staining solution for 1 min, washed with tap water for 10 min, and then immersed in eosin Y (Fuji Film Wako) staining solution for 1 min. The sections were then immersed in 70 % ethanol, 80 % ethanol and 95 % ethanol for 10 s each, followed by three immersions in 100 % ethanol for 10 s each. Finally, the sections were cleared by immersion in xylene three times and then covered with a coverslip using Multi Mount 220 (Matsunami Glass, Osaka, Japan).

2.5. Azan staining

The tissues were fixed in 4 % paraformaldehyde and then used to prepare 4 μm frozen sections. The sections were immersed in Mallory's azocarmine G staining solution (Muto Pure Chemicals, Osaka, Japan) at 50 °C for 30 min, followed by staining at room temperature for an additional 30 min. After washing with tap water, the sections were mordanted in 5 % phosphomolybdic acid solution (Muto Pure Chemicals) for 30 min, washed with running water, and then rinsed with distilled water. Next, the sections were stained with aniline blue-orange G mixture (Muto Pure Chemicals) for 15–30 min and differentiated with 100 % ethanol. Finally, the sections were cleared by immersion in xylene three times for 10 min each and covered with a coverslip using Multi

Mount 220 (Matsunami Glass).

2.6. Bulk RNA sequencing analysis

RNA extraction from the bladder was performed using the RNeasy Mini Kit (Qiagen, Hilden, Germany). Briefly, fresh tissues were minced in RNeasy Lysis Buffer containing β-mercaptoethanol and further homogenized using a 20 G needle and syringe. RNA was then extracted according to the kit's protocol. RNA quantity verification and RNA sequencing were outsourced to Rhelixa (Tokyo, Japan). Libraries were prepared using the NEBNext® Poly(A) mRNA Magnetic Isolation Module (NEB E7490, New England Biolabs, Ipswich, MA, USA) and the NEBNext® Ultra RNA Library Prep Kit (New England Biolabs), generating 150 bp paired-end reads on the Illumina NovaSeq 6000 platform (Illumina, San Diego, CA, USA). Raw sequencing reads were quality controlled using FastQC (v0.11.7), and low-quality bases and adapter sequences were trimmed using Trimmomatic (v0.38). Clean reads were aligned using HISAT2 (v2.1.0), and gene-level read counts were obtained using featureCounts (v1.6.3). Differential expression analysis was performed using DESeq2 (v1.24.0), considering genes with an adjusted *p*-value <0.05 as significantly differentially expressed. Gene ontology enrichment analysis was conducted using goatools (v1.1.6). The sequencing data have been deposited in the DDBJ Sequence Read Archive (Accession number: PRJDB18909).

2.7. RNA extraction and quantitative PCR (qPCR)

RNA extraction was performed using the RNeasy Mini Kit (Qiagen). The quality and concentration of the extracted RNA were assessed using a NanoDrop spectrophotometer (Thermo Fisher Scientific, Waltham, MA, US). The purity of the RNA was confirmed by an A260/A280 ratio in the range of 1.8–2.0. Next, cDNA was synthesized from the extracted RNA. The Revertra Ace qPCR Kit (Toyobo, Osaka, Japan) was used for cDNA synthesis, following the protocol for reverse transcription. qPCR was performed using the synthesized cDNA. The FAST SYBR Green Master Mix (Applied Biosystems, Darmstadt, Germany) was used for qPCR, with the following cycling conditions: initial denaturation at 95 °C for 20 s, denaturation at 95 °C for 3 s, and annealing/extension at 60 °C for 30 s (40 cycles). Gene expression levels for each sample were normalized using 18S rRNA as an endogenous control. The primers used are listed in Table 1. Data analysis was performed using the ΔΔCt method to calculate relative gene expression levels.

2.8. Cell isolation

Lamina propria lymphocytes (LPL) were isolated from the colon. The colons of the mice were harvested, and feces and adipose tissue were removed. The intestine was longitudinally opened and washed with PBS, then placed in Hank's balanced salt solution (HBSS; Nacalai Tesque, Kyoto, Japan) containing 1 mM dithiothreitol (DTT; Wako Pure Chemical, Osaka, Japan) and shaken at room temperature for 15 min. Subsequently, the intestine was transferred to HBSS containing 5 mM ethylenediaminetetraacetic acid (EDTA; Nacalai Tesque) and shaken at 37 °C for 15 min. Next, the tissue was minced in RPMI medium (Nacalai Tesque) containing 4 % fetal bovine serum (FBS; Gibco, Grand Island, NY, USA), and 1 mg/ml collagenase D (Roche Diagnostics, Mannheim, Germany), 40 μg/ml DNase (Roche Diagnostics) and 0.5 mg/ml dispase (Godo Shusei, Chiba, Japan) were added. The mixture was shaken at 37 °C for 40 min and filtered through 40 μm EasyStrainers (Greiner Bio-One GmbH, Frickenhausen, Germany). Following centrifugation at 500 g for 5 min, the supernatant was discarded, and the pellet was resuspended in RPMI containing 10 % FBS and 50 μM 2-mercaptoethanol to prepare the cell suspension.

Bladder tissue was harvested, minced in 250 μl RPMI containing 4 % FBS, 1 mg/ml collagenase, 40 μg/ml DNase and 0.5 mg/ml dispase. The tissue was shaken at 37 °C for 35 min, with 1.25 μl of 0.5 M EDTA added during the last 5 min. After shaking, DNase medium (containing 4 % FBS and 40 μg/ml DNase in RPMI) was added, and the mixture was vortexed, followed by centrifugation at 500 g for 5 min. The supernatant was removed, DNase media was added, and the mixture was pipetted and passed through 40 μm EasyStrainers. After centrifugation at 500 g for 5 min at 4 °C, the supernatant was discarded, and the pellet was resuspended in RPMI containing 10 % FBS and 50 mM 2-ME to prepare the cell suspension.

2.9. Antibody and flow cytometric analysis

The monoclonal antibodies and reagents used for flow cytometric analysis were as follows: perCP-conjugated anti-CD45 (30-F11), FITC-conjugated anti-CD4 (RM4-5), APC-conjugated anti-IFN-γ (XMG1.2), PE-conjugated anti-IL-17A (TC11-18H10.1), IL-17F (9D3.1C8) (16G6) and purified anti-CD16/35 (93) monoclonal antibodies were purchased from Biolegend (San Diego, CA, USA). Cells were stained at 4 °C for 20 min with optimal concentrations of antibodies in flow solution containing 1 % FBS and 5 mM EDTA in a phosphate-based solution. For intracellular staining, cells were stimulated with 50 ng/mL phorbol 12-myristate 13-acetate (PMA; Cayman Chemical, Ann Arbor, MI, USA) and 1 mg/mL ionomycin (IOM; Cayman Chemical) in the presence of GolgiStop™ (BD Biosciences, San Diego, CA, USA) for 4 h, and stained using the BD Cytofix/Cytoperm Kit (BD Biosciences). Stained cells were analyzed using a FACSVerse flow cytometer (BD Biosciences). During data analysis using FlowJo™ software v10 (BD Biosciences), a lymphocyte gate using FSC and SSC gating in flow cytometry was utilized to exclude necrotic cell debris.

2.10. Statistical analysis

Statistical analysis was performed using Prism 5 software (GraphPad, San Diego, CA, USA). An unpaired Student's *t*-test was used to compare the means between two independent groups. Data are expressed as the mean ± standard error of the mean (SEM). A p-value of <0.05 was considered statistically significant.

3. Results

3.1. Colonization of S. oralis in GF mice

To evaluate the inflammatory potential of the commensal bacterium *S. oralis*, GF mice were infected with *S. oralis*, and were maintained and bred in isolators. Since the offspring of *S. oralis*-infected parents were

Table 1
List of primers for quantitative RT-PCR.

Primer for qPCR	Forward (5'−3')	Reverse (5'−3')
Col6a4	GAGCTCTGCAGTACTCTAGGGAAG	GAGTCCGATGCTAGTTGAACTGTC
Col4a1	CTGGCACAAAAGGGACGAG	ACGTGGCCGAGAATTTCACC
Fasn	GGAGGTGGTGATAGCCGGTAT	TGGGTAATCCATAGAGCCCAG
Nqo-1	AGGATGGGAGGTACTCGAATC	AGGCGTCCTTCCTTATATGCTA
Nrf2	GCCCACATTCCCAAACAAGAT	CCAGAGAGCTATTGAGGGACTG
Ho-1	AAGCCGAGAATGCTGAGTTCA	GCCGTGTAGATATGGTACAAGGA
18 s rNRA	CGGCGACGACCCATTCGAAC	GAATCGAACCCTGATTCCCCGTC

sensitized to *S. oralis* from birth, inducing immune tolerance (Knoop et al., 2017), *S. oralis* was considered a commensal bacterium in these offspring. Therefore, the offspring were used as *S. oralis*-colonized mice. First, we confirmed the transmission of *S. oralis* to offspring. *S. oralis* colonized in the oral cavity (colony confirmed by plating mouth wash) and the intestine, including the small intestine (2.1×10^3 cfu/tissue), cecum (2.7×10^5 cfu/tissue) and colon (1.7×10^5 cfu/tissue) in the *S. oralis*-colonized mice, but *S. oralis* was not detected in the blood or bladder. The absence of *S. oralis* detection in the blood suggests that *S. oralis*-colonized mice did not develop infective endocarditis. Throughout the study, *S. oralis* colonization was confirmed in all mice used. These findings suggest that *S. oralis* has the ability to colonize the cecum and large intestine in addition to the oral cavity.

3.2. S. oralis colonization in the intestine causes loose stools

Following the detection of *S. oralis* colonization in the intestine, we analyzed the effect of this bacterium on the intestinal tract. Previously, we showed that *Streptococcaceae* are a minor population in the intestines of CVN mice but a major population in the oral cavity (Nara et al., 2024). Then, we analyzed the presence of *S. oralis* in the oral cavity and intestines of CVN mice by genomic PCR using a primer designed for the *S. oralis rpoB* gene, which encodes the β subunit of bacterial RNA polymerase and a homologous protein in plastids (Tsai et al., 2018). Expectedly, the oral cavity of CVN mice contained *S. oralis* (Supplementary Figure 2). Thus, we used CVN mice as controls to compare against *S. oralis*-colonized mice to analyze the effects of ectopic colonization. First, we examined the fecal condition of *S. oralis*-colonized mice. The feces of *S. oralis*-colonized mice contained significantly more water than those of CVN mice (Fig. 1A and B). The fecal consistency was evaluated using the Bristol stool scale (Lewis and Heaton, 1997). The CVN mice exhibited feces that were type 3 of "like a sausage or snake but with cracks on its surface", while the S. oralis-colonized mice showed feces that were type 4 of "like a sausage or snake, smooth and soft". To elucidate pathological changes in the intestinal tissues, we performed HE staining of the large intestine. However, no histological changes were observed between CVN mice and *S. oralis*-colonized mice (Fig. 1C). Following this, we investigated the effect of *S. oralis* colonization on T cells among the LPL. We isolated LPL from the large intestine of *S. oralis*-colonized mice and examined the production of IL-17 and IFN-γ. The ratio of CD4+IFN-γ+ cells (Th1), among the isolated LPL was significantly reduced in *S. oralis*-colonized mice compared with CVN mice, but there was no difference in the ratio of CD4+IL-17+ cells (Th17) (Fig. 1D). This suggests that inflammation is likely suppressed in the intestinal tract. Therefore, the observed loose stool phenotype is unlikely to be due to intestinal dysfunction.

3.3. S. oralis-colonized mice show urinary disorders

During breeding, the bedding in the cages of *S. oralis*-colonized mice was particularly moist. No symptoms such as inflammation were observed in the intestines of *S. oralis*-colonized mice, so we analyzed their urinary function. First, we examined the number of urinations over 3 h (2–5PM). *S. oralis*-colonized mice urinated significantly more frequently than CVN mice, suggesting symptoms of frequent urination (Fig. 2A), although there was no difference in the total urine volume over 3 h (Fig. 2B). The increased humidity in the bedding of *S. oralis*-colonized mice suggested that a difference in total urine volume might have been observed if the analysis had been conducted over 24 h, considering that mice are nocturnal and urinate most frequently at night (Kira et al., 2017). To investigate the cause of frequent urination in *S. oralis*-colonized mice, Azan staining of bladder tissue was performed (Fig. 3A). Interestingly, the bladder tissues of *S. oralis*-colonized mice were atrophied compared with CVN mice. Furthermore, *S. oralis*-colonized mice showed significant edema and fibrosis of the lamina propria of the bladder mucosa, fibrosis in the detrusor muscle tissue and epithelial desquamation of the bladder mucosa (Fig. 3A). These findings are similar to those reported in IC (Lin et al., 2021), suggesting that *S. oralis*-colonized mice may develop IC. However, no significant infiltration of inflammatory cells was observed in the bladder tissue by HE staining (Supplementary Figure 3). IC has two types: non-Hunner type IC and Hunner type IC, which is characterized by enhanced Th1/17 immune responses (Akiyama et al., 2023). Therefore, we isolated cells from the bladder and examined CD4 T cells localized in

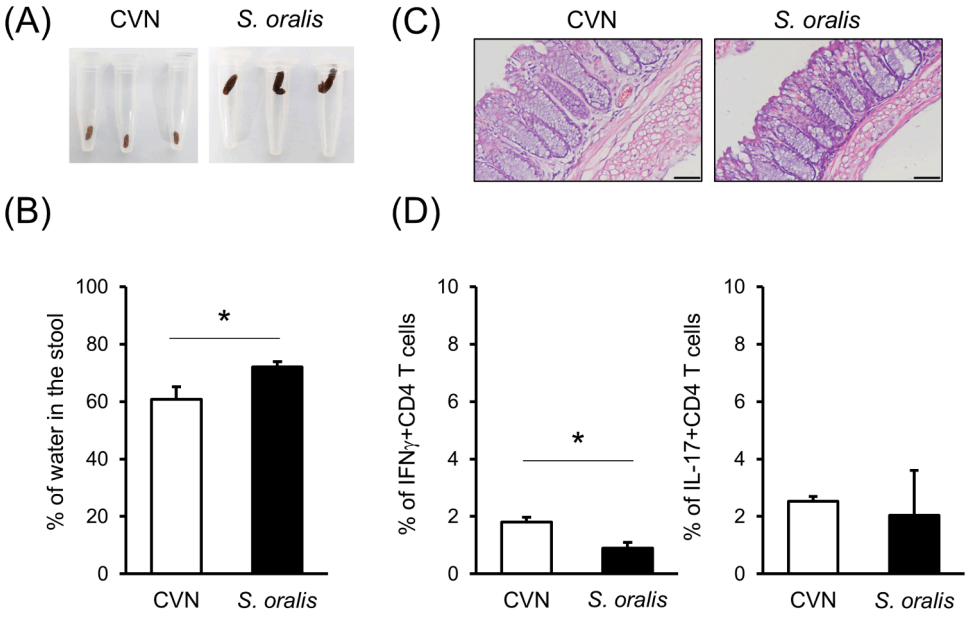

Fig. 1. Analysis of the intestinal tract of *S. oralis*-colonized mice
(A) The feces of CVN mice and *S. oralis*-colonized mice. (B) The water content percentage of feces. *$p < 0.05$ (unpaired Student's *t*-test, CVN $n = 10$, *S. oralis* $n = 8$), data are representative of two independent experiments. (C) Hematoxylin and eosin (HE)-stained images of the intestinal tract from CVN mice and *S. oralis*-colonized mice. Magnification: 40×, scale bar: 50 μm. (D) The percentage of IFN-γ+CD4 T cells and IL-17+CD4 T cells in colonic LPL after stimulation with PMA/IOM. *$p < 0.05$ (unpaired Student's *t*-test, CVN $n = 3$, *S. oralis* $n = 3$), data are representative of three independent experiments.

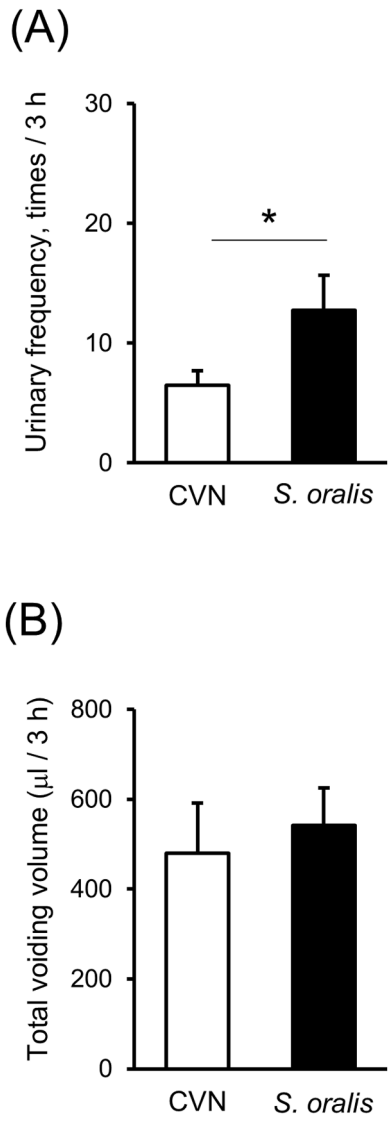

Fig. 2. Analysis of urinary function in *S. oralis*-colonized mice
(A) Urination frequency within 3 h and (B) total urine volume excreted within 3 h in CVN mice and *S. oralis*-colonized mice. *$p < 0.05$ (unpaired Student's *t*-test, CVN $n = 4$, *S. oralis* $n = 4$), data are representative of two independent experiments.

the bladder using flow cytometry (Fig. 3B). In the bladders of *S. oralis*-colonized mice, unlike the results in the intestine, the proportion of Th1 cells was similar to CVN mice. There was no difference in Th17 cells between CVN mice and *S. oralis*-colonized mice. Furthermore, when we examined the production of IFN-γ in urine, IFN-γ was below the detection limit in both *S. oralis*-colonized and CVN mice (data not shown).

3.4. Chronic inflammation in the bladder tissues of S. oralis-colonized mice

To elucidate the mechanisms of bladder fibrosis onset, we performed RNA sequencing analysis using younger mice, which did not exhibit the high moisture in feces and bedding seen in mice aged 22–25 weeks that already showed bladder fibrosis. We investigated the differences in gene expression in the bladder tissues between CVN and *S. oralis*-colonized mice and found distinct gene expression patterns (Fig. 4A). Next, we used gene expression heatmaps to compare the expression patterns of specific gene groups (Fig. 4B). In the bladder tissues of *S. oralis*-colonized mice, the expression of chronic inflammation-related genes (*Ptges, Thbs1, Ccl11, Vcam1*) and extracellular matrix-related genes was higher, whereas the expression of oxidative stress-related genes was lower. Next, we screened for differentially expressed genes using a volcano plot (Fig. 4C). Compared with CVN mice, 276 genes were significantly upregulated, and 87 genes were significantly downregulated in the bladders of *S. oralis*-colonized mice (Table 2).

3.5. Enhanced fibrosis and suppressed antioxidant stress in the bladders of S. oralis-Colonized mice

Gene Ontology (GO) analysis revealed significant changes in several biological processes (BP), cellular components (CC) and molecular functions (MF) in the bladder tissues of *S. oralis*-colonized mice compared with CVN mice (Fig. 5). Regarding BP, extracellular matrix organization, collagen fibril organization and fatty acid synthesis were significantly higher, whereas cellular oxidant detoxification was lower. Regarding CC, the collagen-containing extracellular matrix and extracellular region were significantly higher, whereas oxygen binding and hemoglobin binding were lower. Similarly, regarding MF, the extracellular matrix structural constituent and collagen binding were significantly higer, whereas oxygen-carrying activity and binding were lower. These results suggest that the changes in gene expression in the bladder tissues of *S. oralis*-colonized mice are associated with the upregulation of processes related to fatty acid synthesis, extracellular matrix organization and collagen organization, and the downregulation of processes related to antioxidant stress.

3.6. Gene expression changes in the bladders of S. oralis-Colonized mice

We confirmed the expression of collagen genes (*Col6a4, Col4a1*), fatty acid synthase (*Fasn*), and the antioxidant stress-related gene (*Nqo1*), which were identified by GO analysis, in the bladders of *S. oralis*-colonized mice and CVN mice using qPCR (Fig. 6). The analysis showed that the expression of *Col6a4* was higher in *S. oralis*-colonized mice compared with CVN mice(Fig. 6A). Expression of *Fasn* was slightly higher compared with CVN mice, but the difference was not statistically significant (Fig. 6B). Additionally, expression of the *Nqo1* gene was decreased in *S. oralis*-colonized mice relative to CVN mice (Fig. 6C). These data largely verified the characteristics of the genes identified by bulk RNA sequencing analysis. The expression of the antioxidant-related gene *Nqo1* was significantly lower, but the expression levels of the other antioxidant-related genes, *Nrf2* and *Ho-1*, were unchanged (Supplemental Figure 5).

4. Discussion

In this study, we revealed that the commensal bacterium *S. oralis* induces chronic inflammation and fibrosis in the bladder by intestinal colonization. In the bladder tissue of GF mice, no prominent symptoms such as fibrosis were observed. The ratio of Th1 cells was lower and the ratio of Th17 cells was comparable to those in *S. oralis*-colonized mice (Supplementary Figure 6). This suggests that the bladder fibrosis observed in *S. oralis*-colonized mice is due to *S. oralis* colonization rather than the germ-free status.

Although the exact mechanism of chronic bladder inflammation remains unclear, prolonged exposure to harmful stimuli is known to trigger chronic inflammation (Akiyama et al., 2019). The excessive expression of the chronic inflammation-associated gene *Ptges* may promote the synthesis of prostaglandin E2 (PGE2) and sustain the inflammatory response. Elevated levels of PGE2 have been confirmed in the urine of patients with IC (Wada et al., 2015). Thbs1 has been shown to contribute to impaired bladder function, such as in the case of fibrosis (Long et al., 2024). Thbs1 is included in partial bladder outlet obstruction via the fibroblast growth factor receptor 3 (FGFR3) pathway (Long et al., 2024), and is thought to contribute to chronic inflammatory

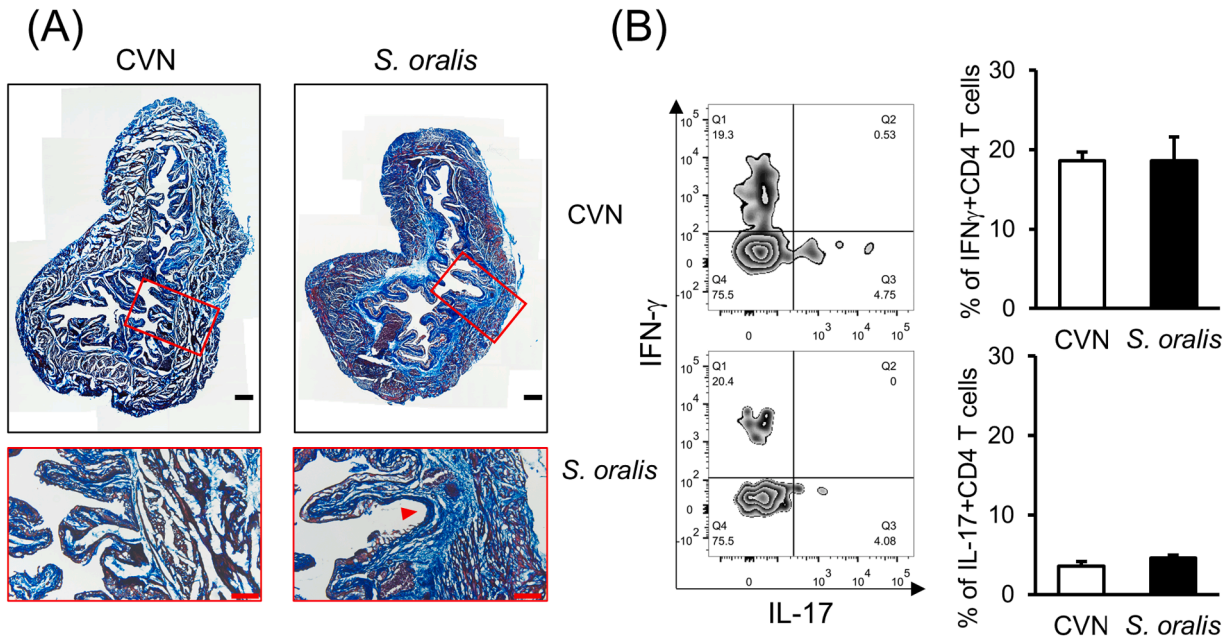

Fig. 3. Histological and immunological analysis of bladder tissue in *S. oralis*-colonized mice and CVN mice
(A) CVN mice and *S. oralis*-colonized mice. The top panel shows the overall view, and the bottom panel shows an enlarged view of the red square area. Blue staining indicates the presence of collagen. Arrowheads indicate epithelial denudation. Magnification: 20×. Black scale bar: 200 μm, red scale bar: 100 μm. (B) The proportion of IFN-γ+CD4 T cells and IL-17+CD4 T cells after stimulation with PMA/IOM in cells isolated from the bladder. The left panel shows dot plots, and the right panel shows the results in a graph. $*p < 0.05$ (unpaired Student's *t*-test, CVN $n = 3$, *S. oralis* $n = 3$). Data are representative of three independent experiments.

responses. Ccl11 is highly expressed in inflammatory bowel diseases such as ulcerative colitis and Crohn's disease, and has been reported to exacerbate inflammation (Polosukhina et al., 2021). Additionally, increased expression of Vcam1 is thought to contribute to the progression of chronic inflammation by promoting the adhesion and migration of leukocytes to the vascular endothelium (Pickett et al., 2023). It has also been suggested that defects in the bladder epithelium and autoimmune responses are related to chronic inflammation (Fallon et al., 2023). Furthermore, regarding bladder fibrosis, studies have reported that repeated inflammation-induced tissue damage and subsequent tissue repair leads to activated fibroblasts that induce excessive collagen production (Kim et al., 2021; Shen et al., 2016). The heatmap results revealed that the colonization of *S. oralis* induces chronic inflammation, which is thought to stimulate fibrosis of the bladder. In addition, GO analysis results indicated the activation of the fatty acid synthesis pathway. Excessive synthesis of fatty acids can induce fibrosis, suggesting that this may also be a stimulatory factor in fibrosis (Hwang and Chung, 2021). Enhanced fatty acid metabolism leads to the synthesis of excessive fatty acids, increasing oxidative phosphorylation in mitochondria, which accumulates reactive oxygen species (ROS) within cells (Schönfeld and Wojtczak, 2008). These findings suggest that, in the bladders of *S. oralis*-colonized mice, fibrosis and ROS accumulation occur, accompanied by enhanced fatty acid synthesis. The accumulation of ROS is believed to exacerbate bladder inflammation and impair bladder function, contributing to the pathogenesis of interstitial cystitis/bladder pain syndrome (IC/BPS) (Mohammad et al., 2024). Thus, the bladders of *S. oralis*-colonized mice harbor impaired antioxidant pathways, leading to insufficient removal of accumulated ROS, which may contribute to IC/BPS-like symptoms. In all experiments, we utilized female mice because male mice did not show any fibrosis in the bladder (Supplementary Figure 4). This observation aligns with the clinical finding that interstitial cystitis often affects women more than men. Therefore, we believe that the findings observed in *S. oralis*-colonized mice are similar to those seen in IC.

The oral *S. oralis* adheres to tooth surfaces by forming a biofilm and produces hydrogen peroxide within these biofilms to prevent the colonization of other bacteria (Zhu and Kreth, 2012). Previous reports have shown that intravesical administration of hydrogen peroxide in mice induces inflammation, including bladder edema and angiogenesis, serving as a model for IC (Homan et al., 2013). On the basis of these findings, hydrogen peroxide derived from *S. oralis* might affect bladder fibrosis. Hydrogen peroxide is produced not only by phagocytes but also by organelles, such as mitochondria, and the endoplasmic reticulum (Dupre-Crochet et al., 2013; Mailloux, 2018; Roscoe and Sevier, 2020). However, because hydrogen peroxide is highly toxic, it needs to be immediately removed by catalase, a hydrogen peroxide reductase expressed in all major tissues, including red blood cells, the liver and kidneys (Glorieux et al., 2015). Considering these factors, *S. oralis* would need to colonize the bladder for hydrogen peroxide to act pathogenically, but no *S. oralis* was detected in the bladder of *S. oralis*-colonized mice in this study.

Th1 cells among the intestinal LPL of *S. oralis*-colonized mice were significantly decreased. A previous study reported that K. *pneumoniae* localization caused an increase in Th1 cells and inflammation in the intestines of GF mice (Atarashi et al., 2017). Therefore, the decrease in Th1 cells in the intestine of *S. oralis*-colonized mice suggests that the presence of *S. oralis* may inhibit intestinal inflammation. On the basis of the finding that the Th17 cells were comparable to those in CVN mice, it may be that the colonization of *S. oralis* is sufficient to induce Th17 cell differentiation in the intestines. In IC, particularly Hunner-type, elevated numbers of Th1 and Th17 cells in the bladder have been reported (Akiyama et al., 2023). However, in *S. oralis*-colonized mice, the proportion of Th1 and Th17 cells in the bladder was similar to that in CVN mice. This was also confirmed by the bulk RNA sequencing results, which showed little increase in the expression of genes involved in the induction of Th1 and Th17 cells. Nevertheless, *S. oralis*-colonized mice showed increased expression of chronic inflammation-related genes, suggesting that inflammation may be maintained through a mechanism different from that of Hunner-type IC.

Urination analysis of mice revealed no difference in the total urine volume in *S. oralis*-colonized mice compared with CVN mice, despite the frequent urination symptoms. This discrepancy might be due to the

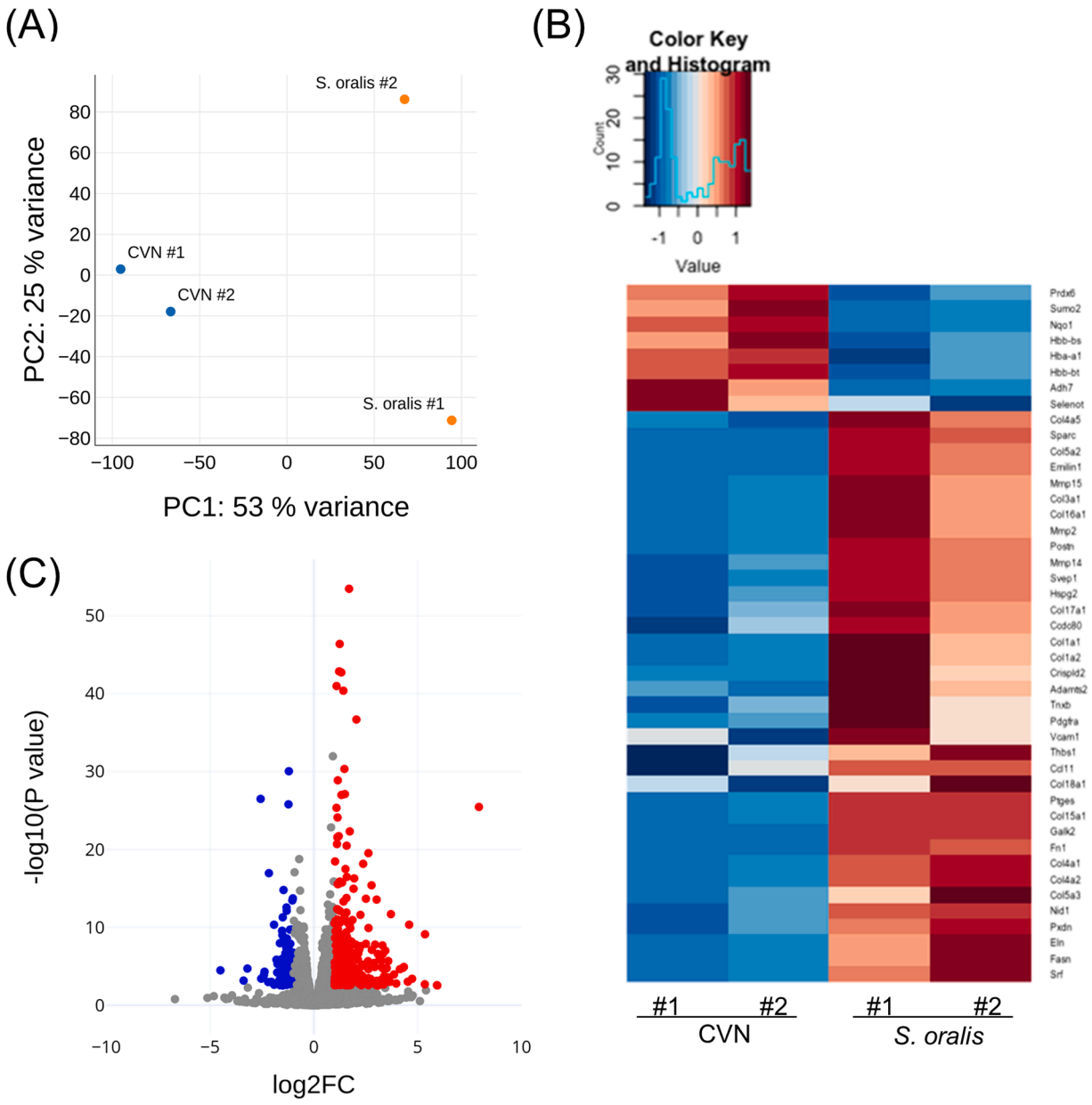

Fig. 4. Impact of *S. oralis* colonization on gene expression in bladder tissue
(A) PCA plot showing clustering between CVN and *S. oralis*-colonized mice samples. (B) Heatmap of differentially expressed transcripts identified from RNA sequencing analysis between CVN mice and *S. oralis*-colonized mice. (C) Volcano plot showing all 363 differentially expressed genes measured by DESeq2 in CVN mice and *S. oralis*-colonized mice. In total, 276 genes were upregulated with a log2 fold change (log2FC) greater than 1 and an adjusted p-value <0.05 (red), and 87 genes were downregulated with a log2FC less than −1 and an adjusted *p* value <0.05 (blue). (CVN $n = 2$, *S. oralis* $n = 2$).

nocturnal behavior of mice, as they urinate most frequently at night rather than during the daytime (Kira et al., 2017). The fact that a higher voiding frequency was observed during the daytime in *S. oralis*-colonized mice clearly indicates the presence of a urination disorder, highlighting the potential impact of *S. oralis* on the urinary system.

5. Conclusion

In this study, we report the novel finding that *S. oralis*, a commensal bacterium present in the oral cavity of mice, can induce cystitis simply by colonizing the intestines of GF mice. Because *S. oralis* also resides in the human oral cavity, the present results not only shed new light on the pathogenicity of *S. oralis* but also suggest the possibility that *S. oralis* may influence the occurrence of human cystitis.

Ethical approval

For animal studies, all applicable international, national and institutional guidelines for the care and use of animals were followed. The animal study protocol was approved by the Institutional Animal Care and Use Committee of Showa University (Approval No. 224,044).

Credit author statement

Natsuno Nakamura: Conducted all experiments, Data curation, Formal analysis, Writing - original draft.

Kota Iioka: Conducted all experiments, Contributed to data collection and analysis.

Hirobumi Morisaki: Contributed to the bacteria experiments, Writing - review & editing.

Table 2
Upregulated and downregulated genes in the volcano plot.

Downregulated genes			Upregulated genes							
Nqo1	Adh7	0610031O16Rik	Serpinf1	Lama2	Lgals12	Hspg2	Cspg4	Cyyr1	Ebf1	Fcor
Gstm3	Gm17494	Gm28437	Car4	Sgk1	Rbp4	Errfi1	Ucp3	Fmod	Gnai1	Slc5a3
Prss16	Hspd1-ps3	Gm33051	Col6a1	Ccn2	Col17a1	Slc2a5	Cdo1	Sdk2	Ntrk3	Mir99ahg
Slc16a12	Gm8129	Gm5869	Sema6b	Vnn3	Fasn	Nos3	Mgll	Pnpla3	Chpt1	4930515G01Rik
Slpi	Gm7331	Gm5905	Gramd1a	Dram1	Pfkfb1	Rbp7	Palmd	Coro2b	Pyroxd2	Gm5627
Cpm	Rps26-ps1	Gm45855	Col1a1	Sycp3	Pnpla2	Klb	Apol6	Acacb	Mfap2	Gm9821
Rgs9	Gm10073	Gm8834	Slc1a5	Col6a2	Col7a1	Cxcl9	Loxl2	Cmklr1	Tnnt3	Mup15
Sumo2	Rpl35a	Gm19810	Nr1h3	Acaca	Adhfe1	Rhof	Lrrn1	Proca1	Myl1	Gm45470
Slc25a48	Rpl26	Gm48583	Angptl4	Fam20a	Col5a2	Col1a2	Ttyh2	Gpr4	Tlr12	Gm45716
Ly6c2	Unc13c	Gm2999	Pon1	Rnf144a	Col3a1	Eln	Scn7a	S1pr1	Ifi27	Gm5182
Adgrf4	mt-Atp6	Gm6789	Prkd1	Pxdn	Opn3	Tfr2	Nxnl1	Kcna5	Hhip	
Gfra3	Rps23rg1		Plin4	Aspa	Prrx1	Adcyap1r1	Ushbp1	Penk	Mup3	
Alas2	Gm12918		Cd36	Per1	Mtarc1	Lrig1	Ssc5d	Lrtm1	Serpina3c	
Prkcq	Gm13192		Lipe	Gstz1	Ppp2r5a	Klf15	Twist1	Igfals	Rps25-ps1	
Elf5	Fbp1		Fosb	Pygl	Pfkfb3	Plbd1	Pknox2	Tent5b	Pi15	
Dab1	Hba-a1		Cp	Bdkrb2	Acvr1c	Timp4	Acss3	Gprc5a	Rpl7a-ps3	
Cda	Plpp4		Mmd	Serpina3n	Col5a1	Sult1a1	Hoxc9	Gchfr	Nr2f1	
Padi2	Klrg2		Col5a3	Irf4	Agpat2	Dgat2	Fstl4	Irs3	Cebpd	
Uchl1	Gm10443		9330159F19Rik	Aspn	Slc43a1	Ern2	Igsf10	Adamts12	Apcdd1	
Ccdc184	Hbb-bt		Nes	Pxdc1	Galk2	Plk1	Cpz	Angptl8	Myo18b	
Bmp10	Bglap3		Sh2b2	Gadd45g	Fam227b	Acsm5	Clca2	Arxes2	Ifi207	
Hsd17b2	Gm16409		Slc1a3	Vcan	Chst1	Mki67	Scd1	Col6a3	Prr16	
Olfm2	Gm12854		Mlxipl	Itih4	Adam33	Tsc22d3	Kcnk2	Arxes1	Ehd2	
Cyp1a1	Gm4294		Nid1	Rgcc	Rassf2	Adrb3	Fam13a	Arl4c	Ankef1	
Car12	Rpl38-ps2		Trpv1	Ephx2	Tgm3	Col4a1	Dusp8	Mchr1	Mup18	
Slc35d2	Gm14303		Atp1a2	Ebf2	Postn	Col4a2	Cldn22	Ffar2	Mup9	
Rpl39-ps	Rps2-ps13		Mc5r	Ppp1r1a	Bche	Dlc1	Npy6r	4732471J01Rik	Tmem182	
Rsph4a	Rpsa-ps9		Fgfrl1	Dgat1	Mme	Ednra	Foxf2	Ppfia2	2610203C22Rik	
Kcne1	Gm13340		Cd163	Gpihbp1	Col11a1	Ucp1	Prc1	Tmem120b	Gm12523	
Pacsin1	Gm14586		G0s2	Gm9747	Enpep	Hp	Tmem120a	Adam12	B4302 19N15Rik	
Dmgdh	Gm13436		Ebf3	Adamts1	Cd1d1	Slc27a1	Mrap	Klf2	Gm3362	
Gpx2	Gm5526		Dhdh	C1qtnf12	Col15a1	Cdh5	Ptger3	Ntrk2	2810430I11Rik	
Ly6k	9530034E10Rik		Hsd11b1	Paqr4	Brinp1	Usp2	Negr1	Hmcn2	Gm13372	
Flrt1	Gm6485		Cd300lg	Pcdh12	Orm3	Nrg4	Maob	Ghr	Gm15587	
Rpl9-ps7	Ugt1a7c		Ybx2	Arap3	Svep1	Cck	Fmo1	Gsdmc4	Ctcflos	
Nlrp10	Gm17189		Sparc	Cidea	Aqp7	Col6a4	Btnl9	Irs1	Gm15270	
Gm9843	Smim22		Acsl1	Pcx	Cdkn2c	Syde1	Col16a1	Clca3a1	Gm12426	
Hbb-bs	Gm10736		Aoc3	Papss2	Cyp4b1	Ablim3	Atp1a3	Cebpb	4930458D05Rik	

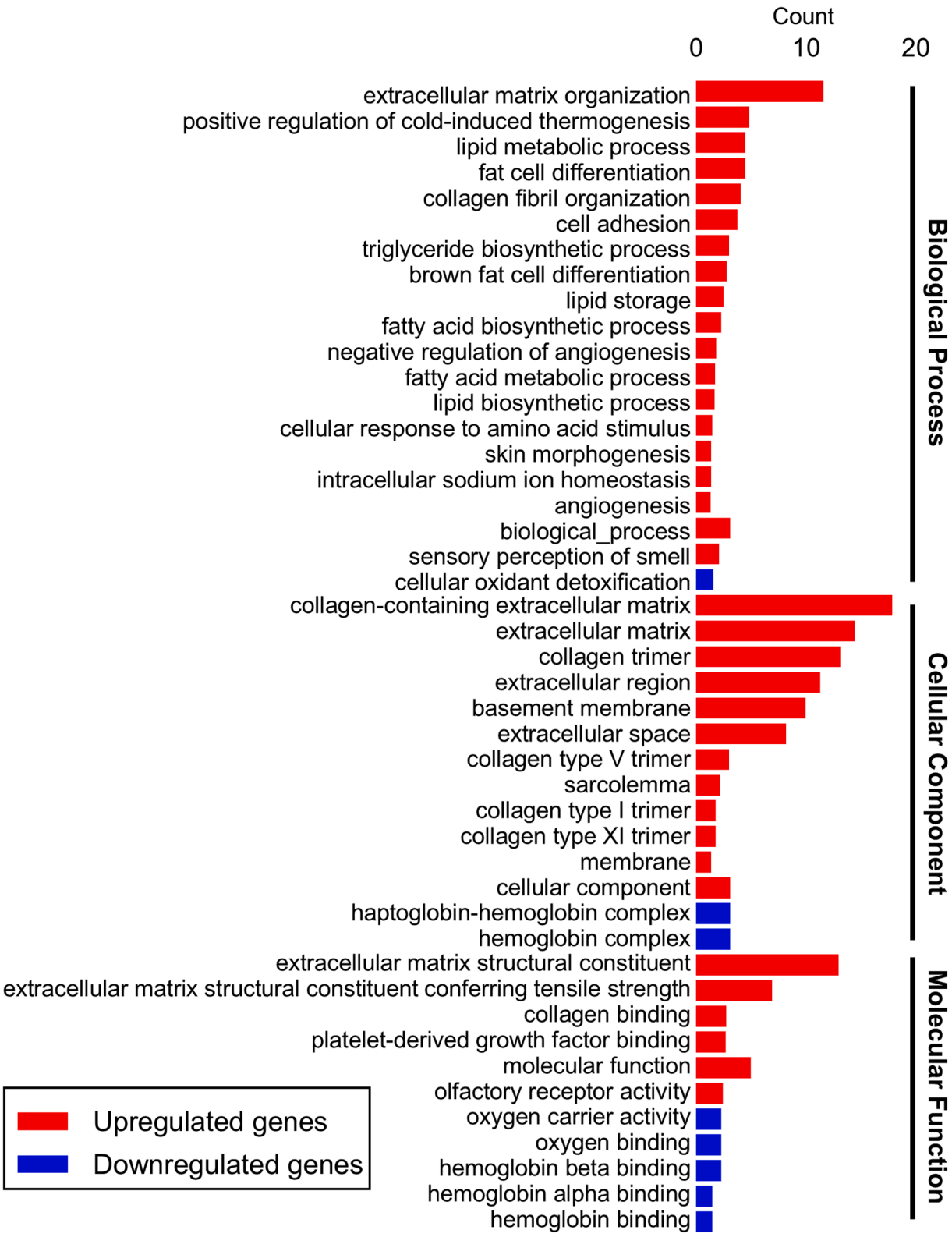

Fig. 5. Pathway and GO analysis in *S. oralis*-colonized mice
Biological Process, Cellular Component, Molecular Function. Red bars indicate upregulated genes with a log2 fold change (log2FC) greater than 1 and an adjusted p-value <0.05, blue bars indicate downregulated genes with a log2FC less than −1 and an adjusted p-value <0.05 (CVN $n = 2$, *S. oralis* $n = 2$).

Nobuo Okahashi: Writing - review & editing.

Mie Kurosawa: Contributed to the tissue staining, Writing - review & editing.

Haruka Fukamachi: Contributed to the bacteria experiments, Writing - review & editing.

Shohei Matsui: Contributed to the RNA sequencing analysis.

Takahiro Funatus: Writing - review & editing.

Hirotaka Kuwata: Conceptualization, Writing - review & editing,

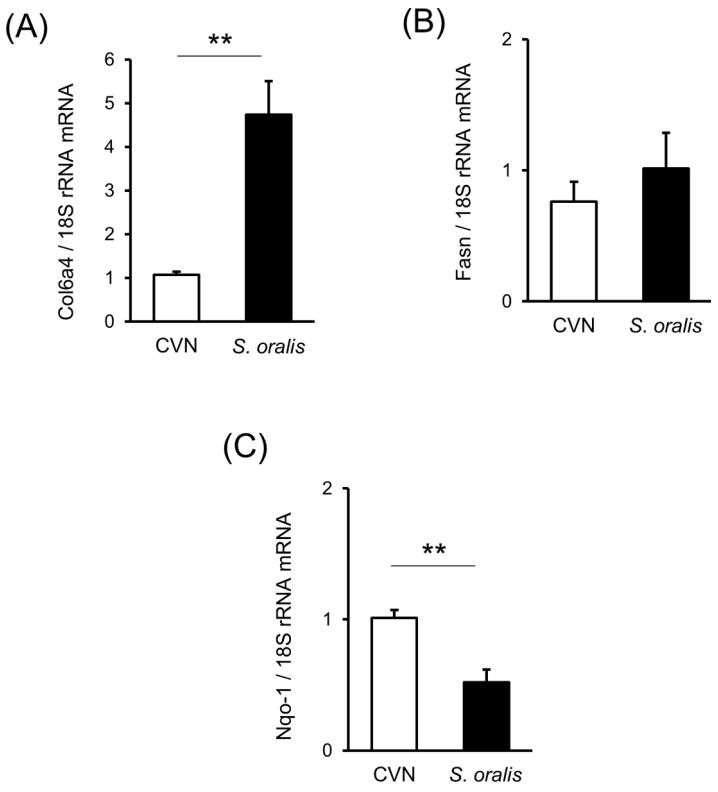

Fig. 6. Q-PCR Analysis of Gene Expression in the Bladder
(A) Comparison of the expression of collagen genes (*Col6a4*) between CVN mice and *S. oralis*-colonized mice. (B) Comparison of fatty acid synthase (*Fasn*) expression between CVN mice and *S. oralis*-colonized mice. (C) Comparison of antioxidant stress-related gene (*Nqo1*) expression between CVN mice and *S. oralis*-colonized mice. $^{**}p < 0.01$ (unpaired Student's *t*-test, CVN $n = 3$, *S. oralis* $n = 3$), data are representative of two independent experiments.

Supervision.

Momoe Itsumi: Conceptualization, Data curation, Formal analysis, Investigation, Project administration, Supervision, Validation, Visualization, Writing - original draft.

Declaration of competing interest

The authors declare that they have no known competing financial interests or personal relationships that could have appeared to influence the work reported in this paper.

Acknowledgments

This research was supported by a Showa University research grant. We would like to express our heartfelt gratitude to Associate Professor Takashi Takaki at the Electron Microscopy Facility of Showa University for his invaluable guidance and support in observing stained tissue sections. RNA sequencing, including RNA library preparation and bioinformatics analysis, was conducted by Rhelixa Inc. (Tokyo, Japan). We also thank Kate Fox, DPhil, and Scott Wysong from Edanz (https://jp.edanz.com/ac) for her assistance in editing a draft of this manuscript.

Supplementary materials

Supplementary material associated with this article can be found, in the online version, at doi:10.1016/j.crmicr.2025.100375.

Data availability

The RNA sequencing data generated and analyzed during the current study are available in the DDBJ repository, under Accession Number PRJDB18909. Additional data that support the findings of this study are available from the corresponding author upon reasonable request.

References

Akiyama, Y., Harada, K., Miyakawa, J., Kreder, K.J., O'Donnell, M.A., Daichi, M., Katoh, H., Hori, M., Owari, K., Futami, K., Ishikawa, S., Ushiku, T., Kume, H., Homma, Y., Luo, Y., 2023. Th1/17 polarization and potential treatment by an anti-interferon-gamma DNA aptamer in Hunner-type interstitial cystitis. iScience 26, 108262. https://doi.org/10.1016/j.isci.2023.108262.

Akiyama, Y., Homma, Y., Maeda, D., 2019. Pathology and terminology of interstitial cystitis/bladder pain syndrome: a review. Histol. Histopathol. 34, 25–32. https://doi.org/10.14670/HH-18-028.

Atarashi, K., Suda, W., Luo, C., Kawaguchi, T., Motoo, I., Narushima, S., Kiguchi, Y., Yasuma, K., Watanabe, E., Tanoue, T., Thaiss, C.A., Sato, M., Toyooka, K., Said, H.S., Yamagami, H., Rice, S.A., Gevers, D., Johnson, R.C., Segre, J.A., Chen, K., Kolls, J.K., Elinav, E., Morita, H., Xavier, R.J., Hattori, M., Honda, K., 2017. Ectopic colonization of oral bacteria in the intestine drives TH1 cell induction and inflammation. Science (1979) 358, 359–365. https://doi.org/10.1126/science.aan4526.

Baty, J.J., Stoner, S.N., Scoffield, J.A., 2022. Oral commensal streptococci: gatekeepers of the Oral cavity. J. Bacteriol. 204, e0025722. https://doi.org/10.1128/jb.00257-22.

Bridge, P.D., Sneath, P.H., 1983. Numerical taxonomy of Streptococcus. J. Gen. Microbiol. 129, 565–597. https://doi.org/10.1099/00221287-129-3-565.

Douglas, C.W., Heath, J., Hampton, K.K., Preston, F.E., 1993. Identity of viridans streptococci isolated from cases of infective endocarditis. J. Med. Microbiol. 39, 179–182. https://doi.org/10.1099/00222615-39-3-179.

Dupre-Crochet, S., Erard, M., Nubetae, O., 2013. ROS production in phagocytes: why, when, and where? J. Leukoc. Biol. 94, 657–670. https://doi.org/10.1189/jlb.1012544.

Ebisutani, N., Fukui, H., Nishimura, H., Nakanishi, T., Morimoto, K., Itou, S., Nakamura, A., Masutani, M., Hori, M., Tomita, T., Oshima, T., Kasahara, E., Sekiyama, A., Miwa, H., 2020. Decreased colonic Guanylin/Uroguanylin expression and dried stool property in mice with social defeat stress. Front. Physiol. 11, 599582. https://doi.org/10.3389/fphys.2020.599582.

Enax, J., Ganss, B., Amaechi, B.T., Schulze Zur Wiesche, E., Meyer, F., 2023. The composition of the dental pellicle: an updated literature review. Front. Oral Health 4, 1260442. https://doi.org/10.3389/froh.2023.1260442.

Fallon, J., Stern, I.T., Laurent, M., Birder, L., Moldwin, R.M., Stern, J.N.H., 2023. The immune system in interstitial Cystitis/Bladder pain syndrome and therapeutic agents. Continence 8, 101057. https://doi.org/10.1016/j.cont.2023.101057.

Fu, K., Cheung, A.H.K., Wong, C.C., Liu, W., Zhou, Y., Wang, F., Huang, P., Yuan, K., Coker, O.O., Pan, Y., Chen, D., Lam, N.M., Gao, M., Zhang, X., Huang, H., To, K.F., Sung, J.J.Y., Yu, J., 2024. Streptococcus anginosus promotes gastric inflammation, atrophy, and tumorigenesis in mice. Cell 187. https://doi.org/10.1016/j.cell.2024.01.004, 882-896 e817.

Glorieux, C., Zamocky, M., Sandoval, J.M., Verrax, J., Calderon, P.B., 2015. Regulation of catalase expression in healthy and cancerous cells. Free Radic. Biol. Med. 87, 84–97. https://doi.org/10.1016/j.freeradbiomed.2015.06.017.

Graves, D.T., Correa, J.D., Silva, T.A., 2019. The oral microbiota is modified by systemic diseases. J. Dent. Res. 98, 148–156. https://doi.org/10.1177/0022034518805739.

Hajishengallis, G., Liang, S., Payne, M.A., Hashim, A., Jotwani, R., Eskan, M.A., McIntosh, M.L., Alsam, A., Kirkwood, K.L., Lambris, J.D., Darveau, R.P., Curtis, M. A., 2011. Low-abundance biofilm species orchestrates inflammatory periodontal disease through the commensal microbiota and complement. Cell Host. Microbe 10, 497–506. https://doi.org/10.1016/j.chom.2011.10.006.

Homan, T., Tsuzuki, T., Dogishi, K., Shirakawa, H., Oyama, T., Nakagawa, T., Kaneko, S., 2013. Novel mouse model of chronic inflammatory and overactive bladder by a single intravesical injection of hydrogen peroxide. J. Pharmacol. Sci. 121, 327–337. https://doi.org/10.1254/jphs.12265fp.

Hwang, S., Chung, K.W., 2021. Targeting fatty acid metabolism for fibrotic disorders. Arch. Pharm. Res. 44, 839–856. https://doi.org/10.1007/s12272-021-01352-4.

Jacobs, K.M., Price, T.K., Thomas-White, K., Halverson, T., Davies, A., Myers, D.L., Wolfe, A.J., 2021. Cultivable bacteria in urine of women with interstitial cystitis: (Not) what we expected. Female Pelvic. Med. Reconstr. Surg. 27, 322–327. https://doi.org/10.1097/SPV.0000000000000854.

Kim, D., Ito, T., Hara, A., Li, Y., Kreth, J., Koo, H., 2022. Antagonistic interactions by a high H_2O_2 -producing commensal streptococcus modulate caries development by Streptococcus mutans. Mol. Oral Microbiol. 37, 244–255. https://doi.org/10.1111/omi.12394.

Kim, S.J., Kim, J., Na, Y.G., Kim, K.H., 2021. Irreversible bladder remodeling induced by fibrosis. Int. Neurourol. J. 25, S3–S7. https://doi.org/10.5213/inj.2142174.087.

Kira, S., Yoshiyama, M., Tsuchiya, S., Shigetomi, E., Miyamoto, T., Nakagomi, H., Shibata, K., Mochizuki, T., Takeda, M., Koizumi, S., 2017. $P2Y_6$-deficiency increases micturition frequency and attenuates sustained contractility of the urinary bladder in mice. Sci. Rep. 7, 771. https://doi.org/10.1038/s41598-017-00824-2.

Knoop, K.A., Gustafsson, J.K., McDonald, K.G., Kulkarni, D.H., Coughlin, P.E., McCrate, S., Kim, D., Hsieh, C.S., Hogan, S.P., Elson, C.O., Tarr, P.I., Newberry, R.D., 2017. Microbial antigen encounter during a preweaning interval is critical for tolerance to gut bacteria. Sci. Immunol. 2, eaao1314. https://doi.org/10.1126/sciimmunol.aao1314.

Lewis, S.J., Heaton, K.W., 1997. Stool form scale as a useful guide to intestinal transit time. Scand. J. Gastroenterol. 32, 920–924. https://doi.org/10.3109/00365529709011203.

Lin, H.Y., Lu, J.H., Chuang, S.M., Chueh, K.S., Juan, T.J., Liu, Y.C., Juan, Y.S., 2021. Urinary biomarkers in interstitial cystitis/bladder pain syndrome and its impact on therapeutic outcome. Diagnostics. (Basel) 12. https://doi.org/10.3390/diagnostics12010075.

Long, J., Yang, Y., Yang, J., Chen, L., Wang, S., Zhou, X., Su, Y., Liu, C., 2024. Targeting Thbs1 reduces bladder remodeling caused by partial bladder outlet obstruction via the FGFR3/p-FGFR3 pathway. Neurourol. Urodyn. 43, 516–526. https://doi.org/10.1002/nau.25366.

Lopez-Medina, E., Fan, D., Coughlin, L.A., Ho, E.X., Lamont, I.L., Reimmann, C., Hooper, L.V., Koh, A.Y., 2015. Candida albicans inhibits Pseudomonas aeruginosa virulence through suppression of Pyochelin and pyoverdine biosynthesis. PLoS. Pathog. 11, e1005129. https://doi.org/10.1371/journal.ppat.1005129.

Mailloux, R.J., 2018. Mitochondrial antioxidants and the maintenance of cellular hydrogen peroxide levels. Oxid. Med. Cell Longev., 7857251 https://doi.org/10.1155/2018/7857251, 2018.

Mohammad, A., Laboulaye, M.A., Shenhar, C., Dobberfuhl, A.D., 2024. Mechanisms of oxidative stress in interstitial cystitis/bladder pain syndrome. Nat. Rev. Urol. 21, 433–449. https://doi.org/10.1038/s41585-023-00850-y.

Nara, M., Kurosawa, M., Itsumi, M., Morisaki, H., Fukamachi, H., Okahashi, N., Suzuki, N., Kuwata, H., 2024. Experimental murine periodontitis increases salivary gland IgA-producing B cells following oral dysbiosis. Microbiol. Immunol. https://doi.org/10.1111/1348-0421.13191.

Pearce, M.M., Hilt, E.E., Rosenfeld, A.B., Zilliox, M.J., Thomas-White, K., Fok, C., Kliethermes, S., Schreckenberger, P.C., Brubaker, L., Gai, X., Wolfe, A.J., 2014. The female urinary microbiome: a comparison of women with and without urgency urinary incontinence. mBio 5. https://doi.org/10.1128/mBio.01283-14 e01283-01214.

Pickett, J.R., Wu, Y., Zacchi, L.F., Ta, H.T., 2023. Targeting endothelial vascular cell adhesion molecule-1 in atherosclerosis: drug discovery and development of vascular cell adhesion molecule-1-directed novel therapeutics. Cardiovasc. Res. 119, 2278–2293. https://doi.org/10.1093/cvr/cvad130.

Polosukhina, D., Singh, K., Asim, M., Barry, D.P., Allaman, M.M., Hardbower, D.M., Piazuelo, M.B., Washington, M.K., Gobert, A.P., Wilson, K.T., Coburn, L.A., 2021. CCL11 exacerbates colitis and inflammation-associated colon tumorigenesis. Oncogene 40, 6540–6546. https://doi.org/10.1038/s41388-021-02046-3.

Qiao, L.D., Chen, S., Yang, Y., Zhang, K., Zheng, B., Guo, H.F., Yang, B., Niu, Y.J., Wang, Y., Shi, B.K., Yang, W.M., Zhao, X.K., Gao, X.F., Chen, M., Tian, Y., 2013. Characteristics of urinary tract infection pathogens and their in vitro susceptibility to antimicrobial agents in China: data from a multicenter study. BMJ Open. 3, e004152. https://doi.org/10.1136/bmjopen-2013-004152.

Roscoe, J.M., Sevier, C.S., 2020. Pathways for sensing and responding to hydrogen peroxide at the endoplasmic reticulum. Cells 9. https://doi.org/10.3390/cells9102314.

Schönfeld, P., Wojtczak, L., 2008. Fatty acids as modulators of the cellular production of reactive oxygen species. Free Radic. Biol. Med. 45, 231–241. https://doi.org/10.1016/j.freeradbiomed.2008.04.029.

Shen, C.H., Wang, S.C., Wang, S.T., Lin, S.M., Wu, J.D., Lin, C.T., Liu, Y.W., 2016. Evaluation of urinary bladder fibrogenesis in a mouse model of long-term ketamine injection. Mol. Med. Rep. 14, 1880–1890. https://doi.org/10.3892/mmr.2016.5482.

Taga, H., Kishida, T., Inoue, Y., Yamamoto, K., Kotani, S.I., Masashi, T., Ukimura, O., Mazda, O., 2023. TGF-beta inhibitor treatment of H_2O_2-induced cystitis models provides biochemical mechanism for elucidating interstitial cystitis/painful bladder syndrome patients. PLoS. One 18, e0293983. https://doi.org/10.1371/journal.pone.0293983.

Tsai, C.Y., Tang, C.Y., Tan, T.S., Chen, K.H., Liao, K.H., Liou, M.L., 2018. Subgingival microbiota in individuals with severe chronic periodontitis. J. Microbiol. Immunol. Infect. 51, 226–234. https://doi.org/10.1016/j.jmii.2016.04.007.

Wada, N., Ameda, K., Furuno, T., Okada, H., Date, I., Kakizaki, H., 2015. Evaluation of prostaglandin E2 and E-series prostaglandin receptor in patients with interstitial cystitis. J. Urol. 193, 1987–1993. https://doi.org/10.1016/j.juro.2015.01.010.

Xu, H., Sobue, T., Bertolini, M., Thompson, A., Dongari-Bagtzoglou, A., 2016. Streptococcus oralis and Candida albicans synergistically activate mu-Calpain to degrade E-cadherin from oral epithelial junctions. J. Infect. Dis. 214, 925–934. https://doi.org/10.1093/infdis/jiw201.

Zhang, B., Zhou, J., Xie, G., Zhang, L., Zhang, Y., Xu, K., Feng, T., Yang, S., 2023. A case of urinary tract infection caused by multidrug resistant Streptococcus mitis/oralis. Infect. Drug Resist. 16, 4285–4288. https://doi.org/10.2147/IDR.S416387.

Zhu, L., Kreth, J., 2012. The role of hydrogen peroxide in environmental adaptation of oral microbial communities. Oxid. Med. Cell Longev., 717843 https://doi.org/10.1155/2012/717843, 2012.